Intercellular Chemical Communication through EV Exchange: Evaluation of the EV Fusion Process Parameters at the Receiving Cell

Alfio Lombardo, Giacomo Morabito, Carla Panarello, Fabrizio Pappalardo

***Abstract*—Cells communicate with each other exploiting a variety of chemical signals. Among them, Extracellular Vesicles (EVs) have attracted large interest by the scientific community. In fact, thanks to the advances in bio-nano-technology and the possibility of engineering EVs, they are envisioned as a perfect means for distributing biological information among receiving cells. However, deciphering the molecular mechanisms that regulate the delivery of EV cargo is, today, a necessary, yet challenging, step toward the exploitation of EV signaling to support innovative and efficient therapeutic protocols, alternative to current drug delivery technologies. In particular, very little information is currently available on the processes of EV fusion, which is the EV internalization process occurring when the EV membrane dissolves into the plasma membrane of the target cell, and the EV content is released into the cytosol. In order to understand the dynamics of this process, this paper introduces an analytical model of the evolution of the fusion process. Moreover, since the measurement of the biological parameters driving the fusion process is far to be achieved, in this paper we use the model as a tool to infer likely values of such parameters from parameters that are measurable with current technology.**

***Index Terms*—Cell-to-cell Communication, Extracellular Vesicle, Mathematical Model, Vesicle Fusion.**

I. Introduction

CELL signalling, in biology, is the ability of biological cells to respond to stimuli and to produce changes in the surrounding environment that other cells can sense and respond to. This complex mechanism is analogous to the information packets exchange in communication networks, where the biological cells represent the transmitting and receiving devices that communicate through physical (e.g. mechanical pressure, voltage, temperature, light) or chemical signals (e.g. molecules, gas) [1].

Among the different types of chemical signals, Extracellular Vesicles (EVs) have attracted particular interest in the scientific community [4], [10], [31]. EVs are nano-sized spherical particles that carry molecules of various natures. They are enveloped by a phospholipid membrane, which shields their content from the external environment [6]. Once secreted by a donor cell, they diffuse into the extracellular space and are received by some target cells through several possible uptake mechanisms [18], as shown in Fig. 1.

The authors are with the Department of Electrical, Electronics and Informatics Engineering (DIEEI), University of Catania, 95125 Catania, Italy (e-mail:alfio.lombardo@unict.it; giacomo.morabito@unict.it; carla.panarello@unict.it; fabrizio.pappalardo@phd.unict.it).

Manuscript received XXXX; revised XXXX.

These characteristics make natural or synthetic-engineered EVs suitable to be engaged, for the treatment of particular diseases, as a carrier for drug delivery to ill cells [9], [14]. To this purpose, the formalization, according to information and communication theory paradigms, of EV exchange between donor and target cells allows to better understand the dynamics and characteristics of such cell communication and accurately supports the development of innovative and efficient therapeutic protocols.

In this context, let us address the processes and functionalities of the cells as receiving devices. As mentioned before, several mechanisms allow cells to internalize the EVs. It is reasonable to expect that the differences between the various EV internalization processes performed by the target cells are related to different functionalities, also producing different effects. As an example, the pathways linked to endocytosis processes (phagocytosis, macropinocytosis, Lipid RAFT, etc.) requires, through a receptor interaction, the internalization of the EVs, which remain unaltered until their metabolization [18], [30]. On the contrary, in the juxtacrine signalling from EVs to nearby cells, the cell response is triggered by the interaction between receptors, without requiring the internalization of the EVs. Further, in the fusion between the membranes of EVs and target cell, pathways are triggered by contact between membranes, while the EV is not internalized as a whole, rather its content is released directly into the cytosol. Clearly, the biological processes and responses activated by the different EV-cell interaction styles may differ between one another. Therefore, a thorough investigation of the possible interplay between competing internalization processes is crucial for biomedical purposes. One of the most investigated uptake mechanisms [17], [28], [33] is the receptor-mediated endocytosis, which relies on the binding between EVs and receptors on the plasma membrane of the target cell. Concurrent to the endocytosis, the protein-mediated fusion of EVs to the plasma membrane of the target cells occurs [22], [27]. This process, which represents a relevant option for successful therapeutic strategies, has only recently received attention and has not yet been thoroughly investigated.

For all the above reasons, in [15] we have presented a mathematical model of the internalization of EVs through the protein-mediated fusion with the plasma membrane of the target cells. Since the evolution of this membrane fusion is well described in literature [22], [26], the different steps of the fusion process can be described through a system of ordinary differential equations, whose parameters are the rates of the

chemical reactions involved in the binding and fusion of EVs, as well as in the recycling/regeneration process of the proteins involved in the process.

Unfortunately, to the best of our knowledge, little information is available about both the identity of the proteins involved in the process, and the parameters regulating the process dynamics. The majority of knowledge about the external surface fusion between EVs and cells comes mainly from the study of either the fusion between two cells or between viruses with cells, which have suggested interesting hypothesis about the identity of the proteins involved in the cell surface fusion of EVs, as well as possible new line of investigation on this topic [11], [22], [27]. Nevertheless, proper meaningful values for the model parameters are still not available.

To overcome this inconvenience, in this paper we initially use the mathematical model to study the influence of the relevant parameters on the EV fusion evolution and provide a frame of reference for future comparisons between numerical solutions and biological experimental measures. After that, we use the model as a tool to infer the range of more likely values for these biological parameter, given some common bio-lab measurements, such as the EV internalization rate in the receiving cell.

The model proposed in this paper is derived with a similar approach to that used in [33], although this one focuses on the EV uptake process through endocytosis. Other models in literature, such as [28], [34], analyze the communication through EV exchange between donor and target cell, by considering the endocytosis as principal uptake mechanism. The model in [29] theoretically investigates the release of EVs from a donor cell. From the best of our knowledge, our model is the first addressing the EV uptake through protein-mediated fusion with the plasma membrane of the target cell.

The paper is organized as follows. In Section II, the fusion of the EVs with the plasma membrane of the target cell is described and the mathematical model of the resulting process, as derived in [15], has been summarized. Moreover, some assumptions and simplifications are applied to the model in order to consider common conditions for in vitro biological experiments. Section III shows and discusses some numerical results obtained by applying the model. Finally, our conclusions are drawn in Section IV.

II. Fusion of EVs with the Plasma Membrane of the Target Cells

In this work, we focus on the fusion of EVs with the plasma membrane of their target cells. Fusion, in general, is a natural event that occurs when two separate portions of membrane approach and fuse into each other. Spontaneous fusion between the membranes of EV and target cell is rare in nature because membranes have positive charge on the external surface [5]. However, in presence of specific proteins on the surface of both EVs and target cells, the charge pushback is overcome thus the fusion of membranes occurs [12], [24]. The proteins that promote the fusion between membranes are called fusogenic proteins (FPs).

The FPs involved in this phenomenon can be of different nature. Note that, contrarily to the well known analogous intracellular fusion process between EVs and cell organelles or membrane-bound cell compartments, where fusion is known to be primarily promoted by SNARE proteins [8], evidence of surface fusion of EVs with target cells has been only recently provided [21]. Therefore, the identity of the proteins involved in this case, is currently unknown and under investigation [2], [3], [16], [19], [20], [22], [23], [25]. In particular, surface proteins belonging to the family of syncytin, which are known to participate in the cell-to-cell fusion, were discovered also on placental trophoblast exosomes (a particular type of EVs), destined to bind and fuse with blood cells [25], which suggests their involvement in the binding and fusion process of the EVs with the target cells [22].

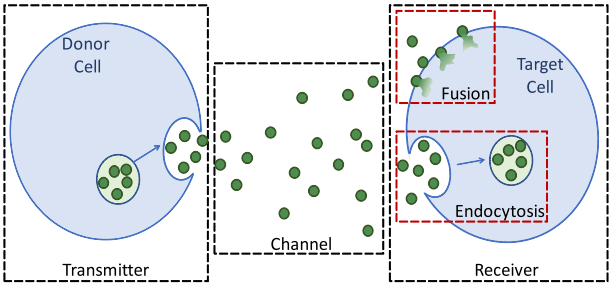

Fig. 1: **Extracellular Vesicle communication system.** On the left, donor cell releases EVs into the extracellular environment. EVs travel thought the cellular matrix and arrive at the target cell, where are internalized through fusion or endocytosis.

However, whatever the nature and identity of the FPs, the evolution of the protein-mediated membrane fusion of EVs with target cells is well described in literature [22], [26]. More specifically, the activation of the fusion process requires at least two pairs of surface FPs (one protruding from the EVs and the other from the plasma membrane of the target cell) [22]. When an EV comes in proximity of the target cell, the high affinity between the FPs results in a bond. At this point, the hydrophobic segments of the bound FPs begin to deepen into the plasma membrane, as described in Fig. 2.

The molecular re-arrangement, together with the re-organization of the closely attached membrane portion of both EV and target cell, takes place, until the dissolution of the membrane segments at the fusion site, i.e. between the two pairs of bound FPs. The EV membrane is, then, inserted in the plasma membrane, which becomes continuous.

Unlike in other simultaneous internalization processes that occur through the cell membrane, such as receptor-mediated endocytosis, where the EVs are internalized with their membrane and, only subsequently, broken down to metabolize their contents, in the fusion the vesicle content is released directly into the cytosol.

A. Fusion Model

In this section, a mathematical model of the EV fusion to the plasma membrane of the target cell is derived, with an approach similar to the one used in [33] to model endocytosis.

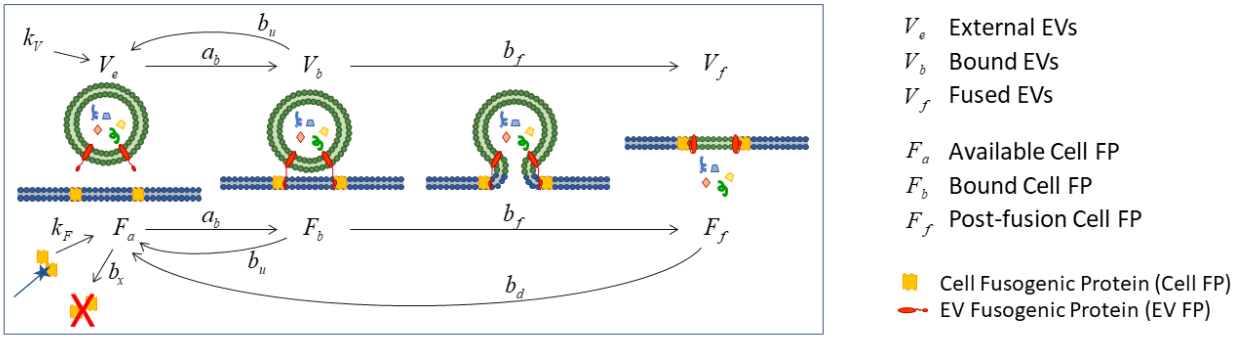

Fig. 2: **EV fusion process.** Two FPs on the EV membrane bind to two FPs on the plasma membrane of the target cell. The FP binding is followed by the re-organization of the closely attached membrane portion of both EV and target cell, until the dissolution of the membrane segments of both EVs and target cells between the two pairs of bound FPs. The EV content is then released into the cytoplasm of the target cell.

Let F be the concentration of FPs on the plasma membrane of the target cell, and let F_a, F_b and F_f denote the concentrations of FPs that are available for binding, currently bound to an EV, and in a post-fusion state, respectively. As already mentioned in Section II, two FPs on the plasma membrane of the target cell are necessary to bind an EV [22], (see also Fig. 2). Therefore, for the sake of simplicity, let us measure F in number of FPs pairs[1] per unit of volume. Further, let V be the concentration of EVs, and let V_e, V_b and V_f denote the concentration of EVs that are in the extracellular space close to the target cell (for brevity, in the following, also called external EVs), currently bound to pairs of FPs, and in a post-fusion state. Near the periphery of the cell, the external EVs initially exhibit a surface sliding behavior until their movements drastically decrease, as an effect of the high affinity between the proteins on the surface of both EVs and cells. The bond between EVs and FPs is, at this point, established [22], which implies that the available FPs, F_a, and the external EVs, V_e, change their state to bound FPs, F_b, and bound EVs, V_b, respectively. This happens at a binding rate constant, a_b, determined, among other factors, by the duration of the surface sliding described above, which depends on the type of FPs and EVs. The binding process described so far, with an approach similar to the one in [33], can be schematized as follows:

$$F_a + V_e \xrightarrow{a_b} F_b + V_b \tag{1}$$

Soon after, the binding between EVs and FPs evolves into fusion, with a rate constant that we denote as b_f. The evolution of EVs from the extracellular space to the EV-cell fusion can be schematized by the following set of reactions, similarly to (1):

$$\{\textit{extracellular medium}\} \xrightarrow{k_V} V_e \underset{b_u}{\overset{a_b}{\rightleftarrows}} V_b \xrightarrow{b_f} V_f \tag{2}$$

[1]In the following we may generically refer to FPs meaning always FPs pairs.

where k_V is the delivery rate of EVs to the cell surface, i.e. the number of EV supplied to the cell by the extracellular medium in the time unit. Note that, a fraction of the EV-FP bonds may disassociate, with a rate constant b_u, before the fusion activation. Therefore, not all the bound EVs evolve into fused ones and the variable V_f counts the EVs whose fusion is successfully completed.

A simple scheme of the EV fusion is illustrated in Fig. 2.

In order to model the evolution of the fusion process, we first focus on the time-dependent concentrations of the available, bound and post-fusion FPs on the cell surface, $F_a(t)$, $F_b(t)$ and $F_f(t)$, respectively, and consider the events that affect their temporal variation. In particular, let us note that the binding of an EV to an available FPs produces a decrease in the concentration of available FPs, $F_a(t)$, and a corresponding increase in the concentration of bound ones, $F_b(t)$. The contribution of this event follows by the application of the law of mass action to the reaction (1). Similarly, the fusion of a bound EV to the plasma membrane, with the rate constant b_f, accounts for a negative contribution in the temporal variation of the bound FPs, $F_b(t)$, and a positive contribution to the temporal variation of the post-fusion FPs, $F_f(t)$.

Besides the binding and fusion events, also the recycling processes of the FPs affect the temporal variation of their concentration and need to be considered [7], [32]. More specifically, it is expected that after the fusion of the EVs is completed, a fraction of the post-fusion proteins becomes again available for binding new EVs, while at the same time old FPs are degraded and new available FPs are produced by the cell. Accordingly, a negative contribution is given to the temporal variation of the post-fusion protein concentration $F_f(t)$ by the recycled proteins with the rate constants b_d. Likewise, the recycled proteins produces a positive contribution in the temporal variation of available proteins concentration $F_a(t)$, whereas the destroyed proteins produce a negative contribution to $F_a(t)$ with a constant rate b_x. Additionally, let

TABLE I: Model parameters

Description	Parameter	Unit of measure
Binding rate constant	a_b	$\text{ml} \cdot \text{mol}^{-1} \cdot \text{h}^{-1}$
Fusion rate constant	b_f	h^{-1}
Bond dissociation rate constant	b_u	h^{-1}
FPs recycling rate constant	b_d	h^{-1}
FPs destroying rate constant	b_x	h^{-1}

$k_F\left(t\right)$ be the production rate of new FPs, i.e. the concentration of new synthesized FPs pairs per time unit, which contributes positively to the concentration $F_a\left(t\right)$.

Finally, the possibility that a fraction of the EV-FP bonds may disassociate before the fusion process is activated, produces, with the rate constant b_u, an increase of the concentration of available FPs, $F_a\left(t\right)$, and a decrease of the bound ones, $F_b\left(t\right)$.

All the above considerations lead to the following equations:

$$\frac{dF_a\left(t\right)}{dt} = k_F\left(t\right) - b_x F_a\left(t\right) + b_d F_f\left(t\right) + \\ + b_u F_b\left(t\right) - a_b F_a\left(t\right) V_e\left(t\right) \tag{3}$$

$$\frac{dF_b\left(t\right)}{dt} = a_b F_a\left(t\right) V_e\left(t\right) - \left(b_f + b_u\right) F_b\left(t\right) \tag{4}$$

$$\frac{dF_f\left(t\right)}{dt} = b_f F_b\left(t\right) - b_d F_f\left(t\right) \tag{5}$$

With similar considerations, let us now focus on the temporal evolution of the concentrations of EVs in the extracellular space close to the target cell $V_e\left(t\right)$, bound to the FPs $V_b\left(t\right)$, and fused to the plasma membrane $V_f\left(t\right)$. By applying the law of mass action to reactions (2), we obtain the following equations:

$$\frac{dV_e\left(t\right)}{dt} = k_V\left(t\right) + b_u V_b\left(t\right) - a_b F_a\left(t\right) V_e\left(t\right) \tag{6}$$

$$\frac{dV_b\left(t\right)}{dt} = a_b F_a\left(t\right) V_e\left(t\right) - \left(b_f + b_u\right) V_b\left(t\right) \tag{7}$$

$$\frac{dV_f\left(t\right)}{dt} = b_f V_b\left(t\right) \tag{8}$$

The set of equations (3)-(8) constitute the system of ordinary differential equations (ODEs) that models the protein-mediated fusion process of EVs to the plasma membrane of a target cell.

B. Initial conditions

In the model presented so far, the variables are the EV and FP concentrations in different phases of the process, and the coefficients are the parameters regulating the processes, i.e. the rates of the chemical reactions involved in EV binding and fusion, as well as in the recycling/regeneration process of the FPs. However, as already said, poor information is available in literature about those parameters. On the contrary, through specific biological experiments, the concentration of the external, bound and fused EVs can be measured over the time, i.e. $V_e(t)$, $V_b(t)$ and $V_f(t)$ can be known. Then, a change of perspective can be applied to the model, so that the Vs are no more unknown variables, and instead the model parameters, together with the concentration of FPs, are the unknowns in the equations (3)-(8). Therefore, we may exploit the model to infer, through a mathematical reverse process, some reasonable values for the model parameters.

Unfortunaltely, to the current state of the art, the experimental measures needed for the above approach are challenging to achieve. In fact, to selectively measure the concentration of the EVs internalized through fusion, the *in vitro* selection or inhibition of specific uptake mechanisms is required. However, technical limitations currently hinder the possibility to efficiently achieve this target. More specifically, the EV-cell interactions involve mechanisms which are physiologically used by cells also for the internalization of other molecules. Therefore the inhibition of some uptake mechanism interferes with the other cellular functions, affecting the normal physiology of the cells, even compromising the cell survival. For these reasons, in this work, we provide a frame of reference for future comparisons between numerical solutions and biological experimental measures, by considering the conditions of common feasible biological experiments, as described in [13], to numerically solve the ODE system (3)-(8).

To this purpose, let us consider the case of a usual *in vitro* experiment where a single dose of EVs is supplied to the target cell at the beginning of the experiments and no other EVs are supplied successively, in the time interval under examination, i.e.:

$$k_V(t) = 0 \tag{9}$$

Moreover we can assume that, in the time interval under examination, the cell dynamics regulating the regeneration of proteins do not introduce, over time, great variations of the concentration of proteins, that is, an equilibrium between old degraded and new produced proteins is maintained. Therefore, in the following we will consider numerical solutions of the ODE system in the case:

$$\begin{aligned} b_x &= 0 \\ k_F(t) &= 0 \end{aligned} \tag{10}$$

Typical initial conditions, at the time instant t_0 (i.e. at the beginning of the observation of the bio-lab experiment), correspond to a situation where the cells have not yet received, i.e. not bound nor internalized, EVs. Therefore, the initial concentration of bound EVs and proteins, as well as fused EVs and post-fused FPs are equal to zero, while the initial concentration of the external EVs and available FPs on the plasma membrane of the target cell is indicated as V_0 and F_0, respectively. This situation is summarized as follows:

$$\begin{cases} V_e\left(t_0\right) = V_0 \\ V_b\left(t_0\right) = 0 \\ V_f\left(t_0\right) = 0 \\ F_a\left(t_0\right) = F_0 \\ F_b\left(t_0\right) = 0 \\ F_f\left(t_0\right) = 0 \end{cases} \tag{11}$$

where the initial concentrations V_0 of external EVs is assigned during the biological experiment planning, whereas the initial concentration F_0 of FPs is unknown. Therefore, in order to make the numerical results independent from the initial concentration of proteins, let us normalize the concentration of all Fs and Vs to the initial concentration of available proteins

F_0. So doing the solutions of the ODE system in (3)-(8), can be analyzed in terms of the ratio $\frac{V_0}{F_0}$. To the purpose, let us denote as

$$S(t) = (F_a(t), F_b(t), F_f(t), V_e(t), V_b(t), V_f(t)) \tag{12}$$

the generic solution of the ODE system in (3)-(8), and with calligraphic letters the normalization of (12) with respect to the concentration of proteins F_0, i.e.:

$$\begin{aligned} \mathcal{S}(t) &= (\mathcal{F}_a(t), \mathcal{F}_b(t), \mathcal{F}_f(t), \mathcal{V}_e(t), \mathcal{V}_b(t), \mathcal{V}_f(t)) = \\ &= \left(\frac{F_a(t)}{F_0}, \frac{F_b(t)}{F_0}, \frac{F_f(t)}{F_0}, \frac{V_e(t)}{F_0}, \frac{V_b(t)}{F_0}, \frac{V_f(t)}{F_0} \right) \end{aligned} \tag{13}$$

Note that, due to the presence in the system (3)-(8) of the non-linear term $F_a V_e$, the normalization $\mathcal{S}(t)$ of the initial condition (11) is solution of the ODE system as long as we redefine, under the considered assumptions, a_b as α_b, as follows:

$$\alpha_b = a_b F_0 \tag{14}$$

The equivalent initial conditions, in this case are:

$$\begin{cases} \mathcal{V}_e(t_0) = \mathcal{V}_0 \\ \mathcal{V}_b(t_0) = 0 \\ \mathcal{V}_f(t_0) = 0 \\ \mathcal{F}_a(t_0) = \mathcal{F}_0 \\ \mathcal{F}_b(t_0) = 0 \\ \mathcal{F}_f(t_0) = 0 \end{cases} \tag{15}$$

where:

$$\begin{aligned} \mathcal{V}_0 &= \frac{V_0}{F_0} \\ \mathcal{F}_0 &= \frac{F_0}{F_0} = 1 \end{aligned} \tag{16}$$

III. Analysis of the ODE solutions

In this section, we will discuss the numerical results of the ODE system, in a time interval of 72 hours, for different orders of magnitude of the model parameters. More specifically, in Section III-A we will investigate the effects of the model parameters on the time evolution of the fusion process. In particular, we will focus on the *basic* fusion process, without considering possible EV-FP bond disassociation, i.e. for $b_u = 0$. The impact of $b_u \neq 0$ will be examined in Section III-B. In Section III-C, we will formally define the internalization rate and evaluate it for a wide range of values of relevant parameters. Finally in Section III-D, we will provide a discussion regarding what are most likely parameter values associated to the measured internalization rate.

For the sake of simplicity, in the following, we will refer to the parameter values without specifying the measurement units, which are meant to be as specified in Table I.

A. Temporal evolution of FP and EV concentrations

First, let us consider the effects of the parameters α_b, b_f and b_d, regulating the *basic* fusion process, without considering possible EV-FP bond disassociation, i.e. $b_u = 0$. In Fig. 3, the time evolution of the concentration of FPs and EVs is shown, in a time interval of 72 hours, for different values of the above mentioned model parameters[2].

Let us initially focus on Fig. 3c, where the temporal evolution of the concentrations $\mathcal{F}_a(t)$, $\mathcal{F}_b(t)$ and $\mathcal{F}_f(t)$, for different values of the binding rate constant α_b, are shown, when the fusion rate constant b_f is equal to 10 and the FP recycling rate constant b_d is 1000. In the small box inside the figure, the 18 minutes after the time instant $t = 0$ is analyzed more in details. As shown in these figures, the concentration $\mathcal{F}_a$ of available FPs is, at the time instant $t = 0$, equal to 1, which represents the total concentration of proteins (see (15) and (16)). Soon after, it rapidly decreases, while the concentration $\mathcal{F}_b$ of bound FPs increases complementary to $\mathcal{F}_a$, meaning that the bond between FPs and EVs is taking place. As expected, for lower values of the binding rate constant α_b (e.g. $\alpha_b = 0.1$, solid lines in Fig. 3c), the concentration $\mathcal{F}_a$ decreases until it reaches about half of the initial concentration of proteins, which is a relatively large value in comparison to the concentration obtained for greater values of α_b, (e.g. $\alpha_b = 100$, dotted lines in Fig. 3c), which instead is close to zero. In fact, low binding rate constants imply (for equal concentrations of reactants) large time intervals where the FPs remain available, waiting for a successful EV-FP bond. On the contrary, the larger the binding rate constant α_b, the shorter the time period the FPs remain available. Therefore, for low binding rate constants, the average over time of the concentration $\mathcal{F}_a$ of available proteins is larger, with respect to the case of high binding rate constants.

After this first rapid decrease, the concentration $\mathcal{F}_a$ increases. The slope of such an increment is sensibly dependent on the value of the binding rate constant α_b. More specifically, for high values of α_b, the concentration $\mathcal{F}_a$ increases slowly, for about the first 10 hours, to steeply increase and stabilize to the initial concentration of FPs. This time interval before the concentration of $\mathcal{F}_a$ stabilizes to the initial concentration of FPs, corresponds to the internalization period, i.e., the duration of the whole internalization process, as shown also in Fig. 3d, where the concentrations $\mathcal{V}_e$ and $\mathcal{V}_f$ of external and fused EVs, respectively, are drawn. Indeed, when $\mathcal{F}_a$ stabilizes around 1 (e.g., about 10 hours for high values of α_b), the concentration $\mathcal{V}_e$ of external EVs to be internalized is close to zero, while the concentration $\mathcal{V}_f$ of fused EVs is close to the initial concentration of EVs.

Let us now compare Fig. 3e to Fig. 3c, where only the recycling rate constant b_d changes, i.e., it decreases by one order of magnitude. As shown in the figures, the internalization period does not change appreciably. In this time interval, the concentration of $\mathcal{F}_f$ appears to be greater when $b_d = 100$ than when $b_d = 1000$. This happens because a slower recycling

[2]In Fig. 3, some curves stop earlier than 72 hours. This happens because, for computational reasons, the calculation of the ODE system solutions automatically stops once the concentration of external EV becomes zero.

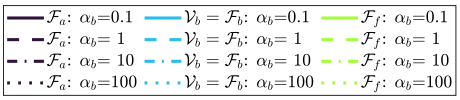

(a) FPsLegend

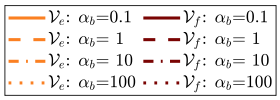

(b) EVsLegend

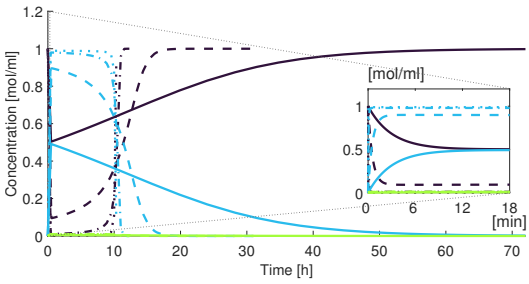

(c) FPs $b_f = 10$, $b_d = 1000$, $b_u = 0$

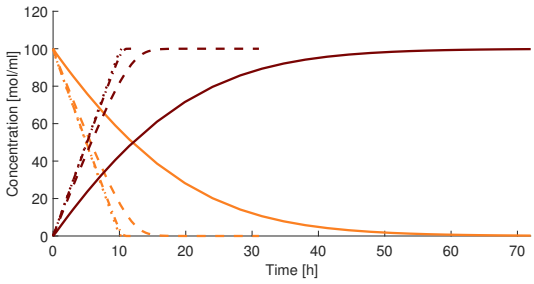

(d) EVs $b_f = 10$, $b_d = 1000$, $b_u = 0$

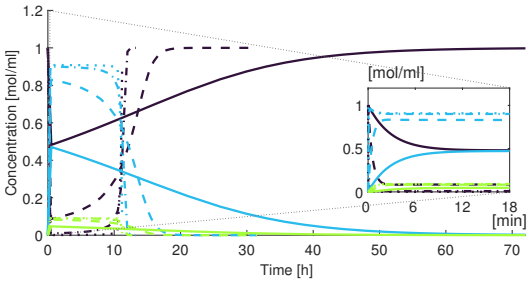

(e) FPs $b_f = 10$, $b_d = 100$, $b_u = 0$

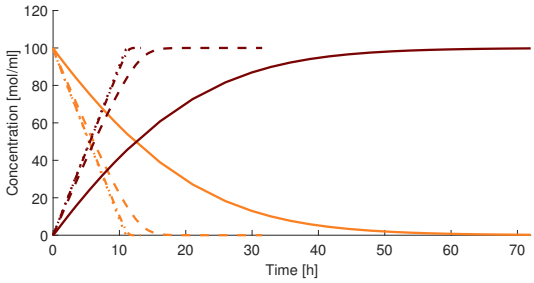

(f) EVs $b_f = 10$, $b_d = 100$, $b_u = 0$

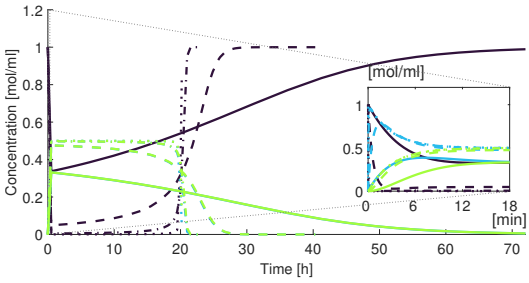

(g) FPs $b_f = 10$, $b_d = 10$, $b_u = 0$

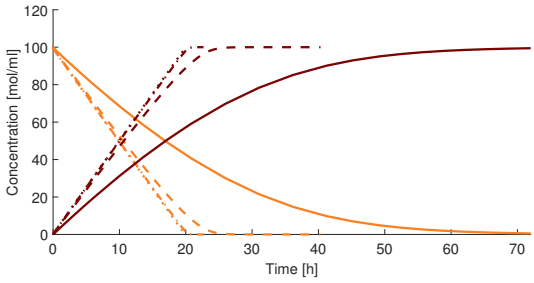

(h) EVs $b_f = 10$, $b_d = 10$, $b_u = 0$

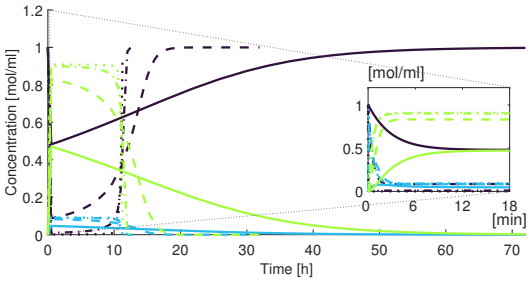

(i) FPs $b_f = 100$, $b_d = 10$, $b_u = 0$

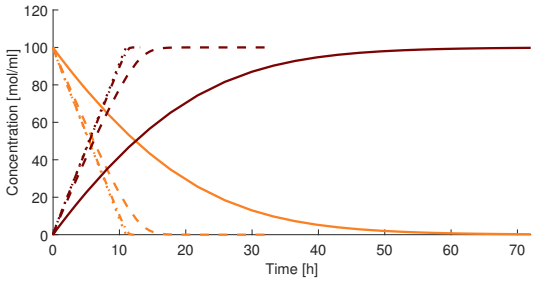

(j) EVs $b_f = 100$, $b_d = 10$, $b_u = 0$

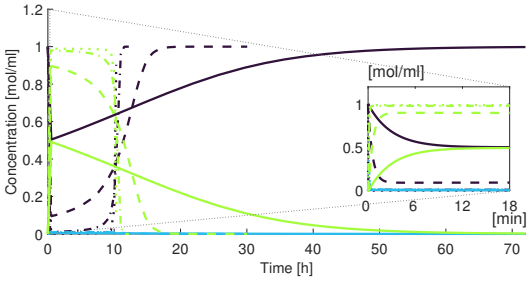

(k) FPs $b_f = 1000$, $b_d = 10$, $b_u = 0$

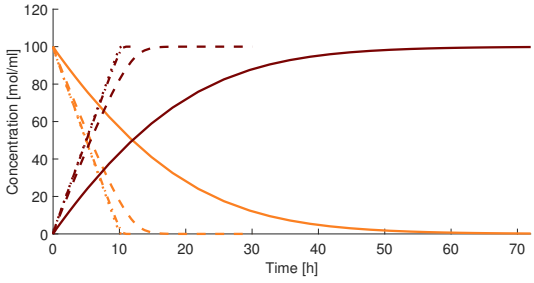

(l) EVs $b_f = 1000$, $b_d = 10$, $b_u = 0$

Fig. 3: Concentration of FPs and EVs for different values of parameters. ($b_u = 0$)

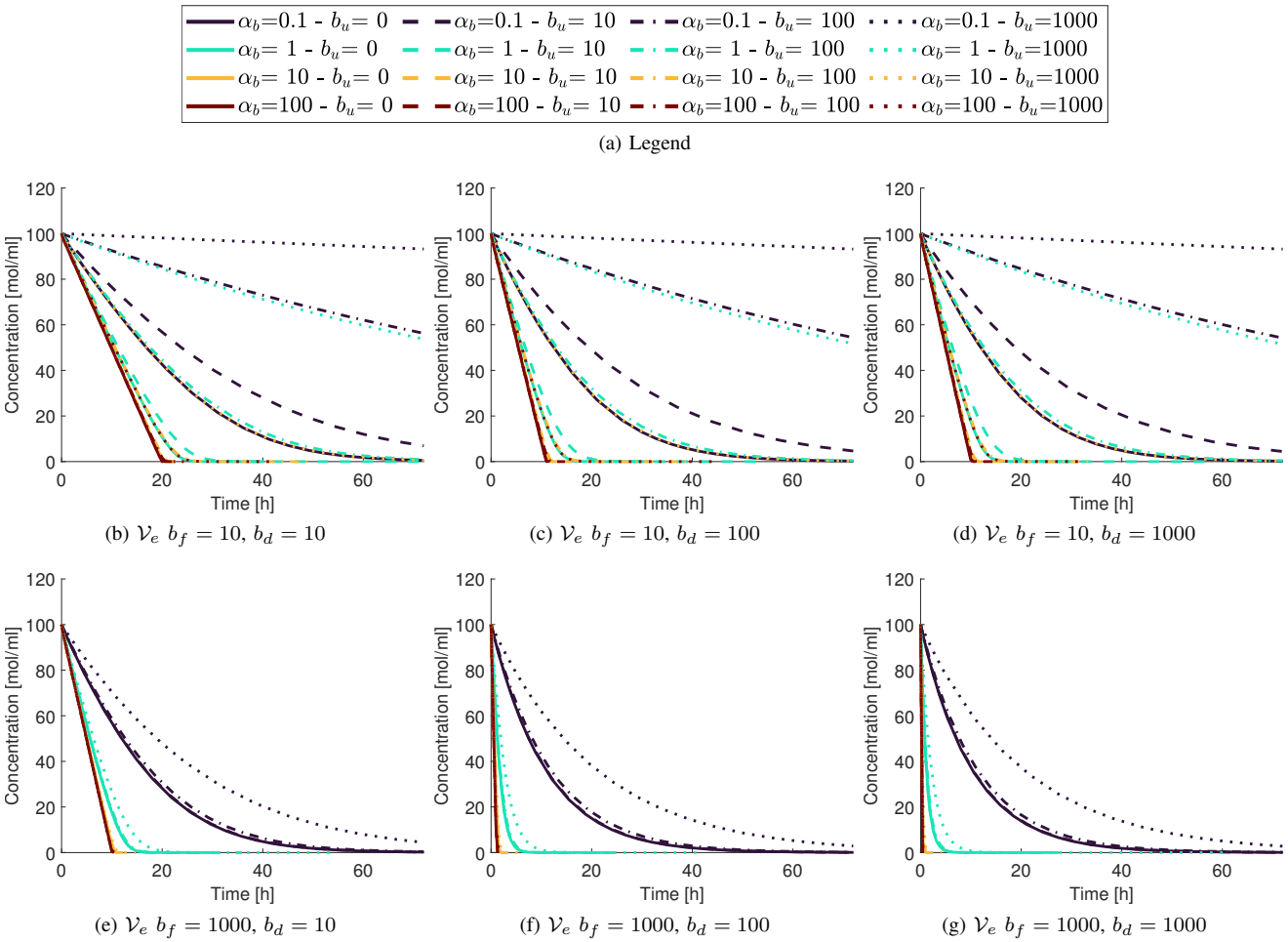

(a) Legend

(b) $\mathcal{V}_e$ $b_f = 10$, $b_d = 10$ (c) $\mathcal{V}_e$ $b_f = 10$, $b_d = 100$ (d) $\mathcal{V}_e$ $b_f = 10$, $b_d = 1000$

(e) $\mathcal{V}_e$ $b_f = 1000$, $b_d = 10$ (f) $\mathcal{V}_e$ $b_f = 1000$, $b_d = 100$ (g) $\mathcal{V}_e$ $b_f = 1000$, $b_d = 1000$

Fig. 4: Concentration of $\mathcal{V}_e(t)$ for different values of parameters

rate constant, introduces a recycling delay, which means that the proteins, that completed successfully the EV fusion, need more time to become again available for binding new EVs. Again, a longer permanence in the fused state, corresponds to a larger average over time of the concentration of fused proteins. As a counter part, since the total concentration of proteins is assumed to be constant in our analysis, such an increase of fused proteins should correspond to a decrease of available and bound proteins. However, as shown in the figures, the concentration $\mathcal{F}_a$ does not show appreciable variations with respect to the previous case, especially for high values of the binding rate constant α_b. This happens because the new available proteins are soon involved in new EV-FP bonds, so maintaining $\mathcal{F}_a$ low. Therefore, the increase of $\mathcal{F}_f$ mainly produces a decrease of the average concentration $\mathcal{F}_b$ of bound FPs. A comparison between Fig. 3d and Fig. 3f shows that the concentrations $\mathcal{V}_e$ and $\mathcal{V}_f$ of external and fused EVs, respectively, are not affected by b_d variations significantly.

When b_d is further reduced to 10, as in Fig. 3g and Fig. 3h, the recycling delay, introduced before the fused proteins become again available, has a higher impact on both $\mathcal{F}_a$ and $\mathcal{F}_b$[3]. More specifically, the concentration of $\mathcal{F}_b$ decreases significantly as $\mathcal{F}_f$ increases, whereas the concentration of $\mathcal{F}_a$ remains quite as low as in the previous considered cases. However, the internalization time is almost doubled, with respect to previous analyzed cases.

Let us now maintain b_d constant and consider an increment of b_f, corresponding to a faster fusion process. By comparing Fig. 3g and Fig. 3h to Fig. 3i and Fig. 3j, the concentration $\mathcal{F}_b$ reduces while the concentration $\mathcal{F}_f$ increases, as b_f grows. The concentration of $\mathcal{F}_a$ is not noticeably affected by the variation of b_f during the internalization time, but the internalization time decreases and the slopes of $\mathcal{V}_e$ and $\mathcal{V}_f$ increase, accordingly. The same trend appears by further increasing b_f, as shown in Fig. 3k and Fig. 3l. Note that increasing b_f and reducing b_d, symmetrically with respect to the case $b_d = b_f$, produces analogous results as of $\mathcal{F}_a$, $\mathcal{V}_e$ and $\mathcal{V}_f$, while swapping the trends of $\mathcal{F}_b$ and $\mathcal{F}_f$, that is, the distribution among bound and fused protein $\mathcal{F}_b$ and $\mathcal{F}_f$ changes in favor of the first or the second, depending on whether the ratio $\frac{b_f}{b_d}$ decreases or increases.

B. Impact of model parameters on the concentration of internalized EVs

In this section we focus on the concentration $\mathcal{V}_e$. Let us explain the reason of this choice. The variable that is usually

[3]Note that in Fig. 3g, the blue lines associated to $\mathcal{F}_b$ are not visible because they are almost perfectly overlapped with the green ones, associated to $\mathcal{F}_f$.

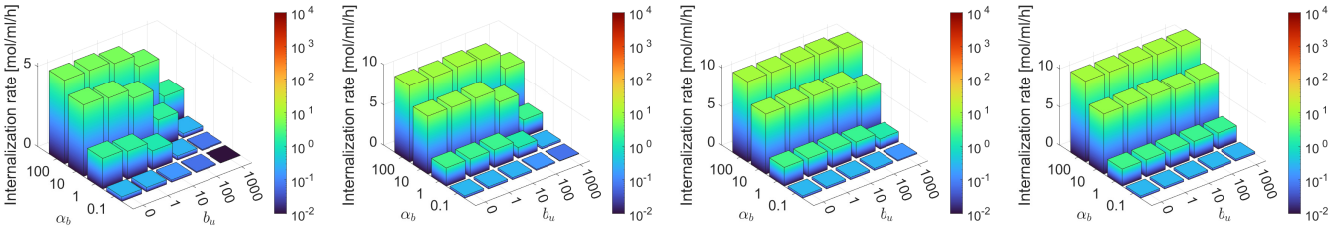

(a) $b_f = 10$, $b_d = 10$ (b) $b_f = 100$, $b_d = 10$ (c) $b_f = 1000$, $b_d = 10$ (d) $b_f = 10000$, $b_d = 10$

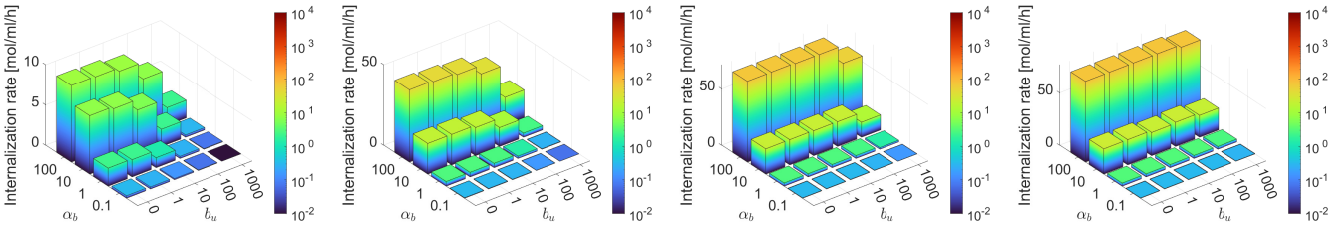

(e) $b_f = 10$, $b_d = 100$ (f) $b_f = 100$, $b_d = 100$ (g) $b_f = 1000$, $b_d = 100$ (h) $b_f = 10000$, $b_d = 100$

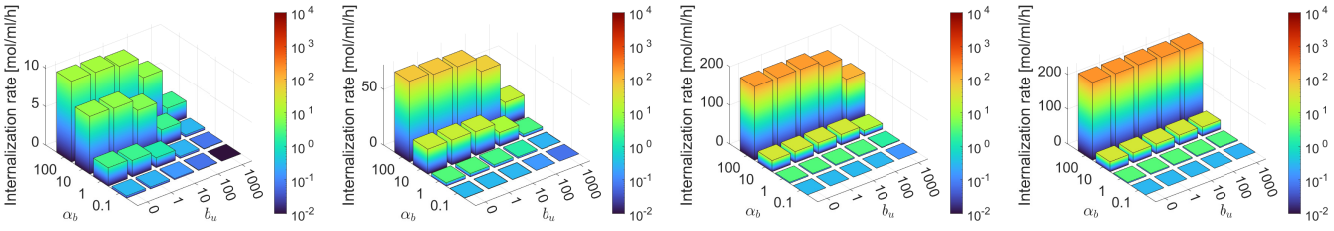

(i) $b_f = 10$, $b_d = 1000$ (j) $b_f = 100$, $b_d = 1000$ (k) $b_f = 1000$, $b_d = 1000$ (l) $b_f = 10000$, $b_d = 1000$

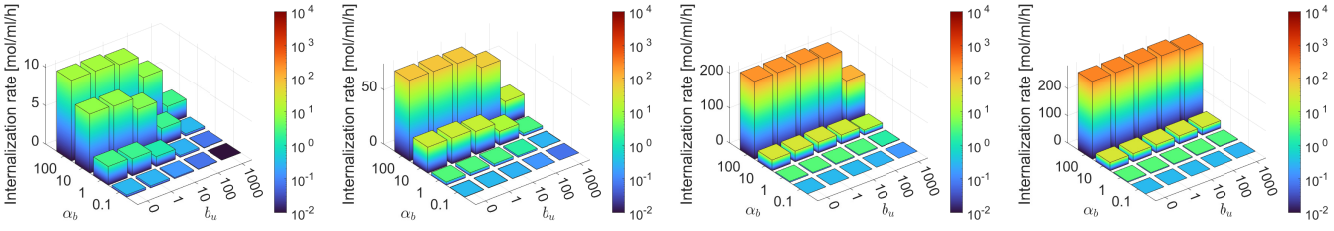

(m) $b_f = 10$, $b_d = 10000$ (n) $b_f = 100$, $b_d = 10000$ (o) $b_f = 1000$, $b_d = 10000$ (p) $b_f = 10000$, $b_d = 10000$

Fig. 5: Internalization rate for $\mathcal{V}_0 = 10$

most accessible to measure in bio-labs experiments is the sum of the EVs internalized (i.e. fused EVs $\mathcal{V}_f$) and still attached to the cell membrane (i.e. bounds EVs $\mathcal{V}_b$). Moreover, an interesting metric for the future applications of this study is the internalization rate, which may be inferred, again, by the analysis of $\mathcal{V}_b + \mathcal{V}_f$. Since we are considering the case where no additional EVs are supplied to the cells in the time interval under examination, the total concentration of EVs (i.e. the sum of external, bound, and fused EVs, $\mathcal{V}_e(t)$, $\mathcal{V}_b(t)$, and $\mathcal{V}_f(t)$ respectively) is constant and equal to the initial concentration $\mathcal{V}_0$ of external EVs. Threfore, the sum of bound and fused EVs, $\mathcal{V}_b + \mathcal{V}_f$ is complementary to the concentration $\mathcal{V}_e$ of external EVs, with respect to $\mathcal{V}_0$. So, for the sake of simplicity, we will focus on a single variable $\mathcal{V}_e$, instead of the sum $\mathcal{V}_b + \mathcal{V}_f$, keeping in mind that the results apply to them equivalently.

In Section III-A we have already glimpsed how the model parameters α_b, b_f and b_d influence the evolution of $\mathcal{V}_e$. More specifically, it is possible to infer that increasing values of the binding rate constant α_b, produce an increase of the slope of $\mathcal{V}_e$ and reduce the internalization period. The same trend appears by increasing b_f and/or b_d. Let us now, analyze the impact of the EV-FP bond disassociation rate constant b_u. This parameter measures the possibility that the bonds between EVs and FPs disassociate before the fusion takes place. When this event occurs, the FPs involved in the bond move from the state *bound* to the state *available*, and the same occurs for the EVs. Therefore, intuitively we expect that increasing the values of b_u for given binding rate constants α_b produces the same effects of lower binding rate constants with $b_u = 0$. This intuition is confirmed by the analysis of Fig. 4, where it can be seen how the slope of $\mathcal{V}_e$ reduces and the internalization time increases, as b_u grows.

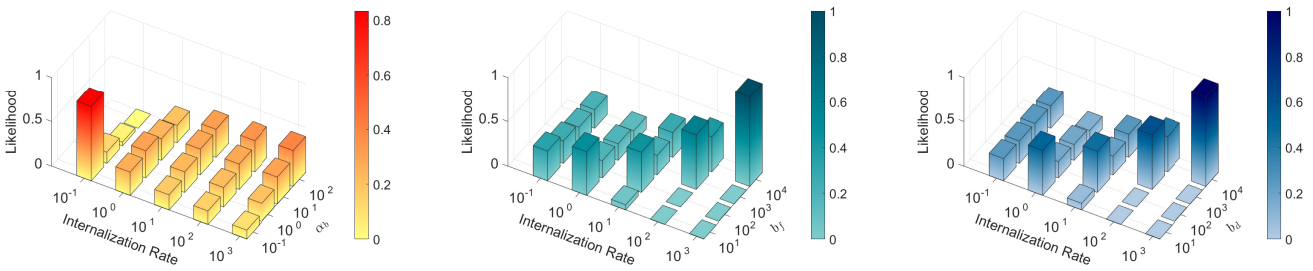

(a) Distribution of the model parameter $\alpha_b$given the Internalization Rate (b) Distribution of the model parameter $b_f$given the Internalization Rate (c) Distribution of the model parameter $b_d$given the Internalization Rate

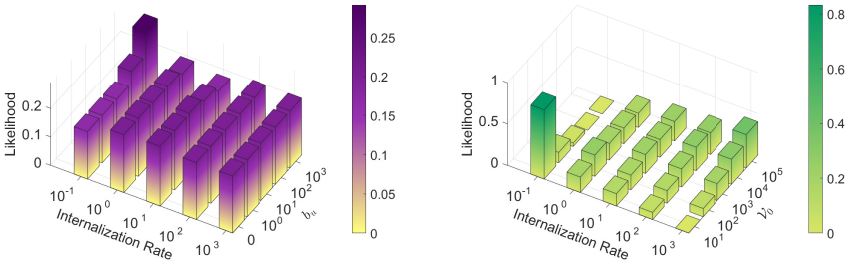

(d) Distribution of the model parameter $b_u$given the Internalization Rate (e) Distribution of the model parameter $\mathcal{V}_0$given the Internalization Rate

Fig. 6: Likelihood of the model parameter values given the Internalization Rate

C. Internalization Rate

In this section, let us focus on the internalization rate, which may be defined as the slope of $\mathcal{V}_e$. Since $\mathcal{V}_e$ shows in general a non linear decrease, its slope changes according to the time instant when we measure it. Therefore, let us define the average internalization rate at 95%, $r_{95\%}$, as follows:

$$r_{95\%} = \frac{0.95\mathcal{V}_0}{t_{95\%}} \tag{17}$$

where $t_{95\%}$ is the time instant where the 95% of the initial external EVs have been internalized.

Fig. 5 shows the internalization rate $r_{95\%}$ for different values of the fusion parameters α_b, b_f, b_d, b_u and defined as in (16).

As expected, the figures show that the internalization rate increases when the binding rate α_b increases, and decreases for increasing values of the bond disassociation rate, b_u. The impact of b_u is however lighter. As far as the fusion rate constant, b_f, and the recycling rate constant, b_d, are concerned, the internalization rate increases as both parameters assume higher values. The analysis of the cases where the initial concentration ratio is $\mathcal{V}_0 = \{100, 1000, 10000\}$, has confirmed the same results.

D. Parameter inference

In this section we elaborate on the most likely EV fusion process parameter values associated to an internalization rate measured in a bio-lab experiment, in the assumption of uniform distribution of the parameter values.

In particular Fig. 6 shows, for each parameter, the likelihood distribution of the parameter values for given order of magnitude of the measured internalization rate. In Fig. 6a we can infer that if the measured internalization rates is in the order of 10^{-1} , than the values of α_b is in the order of 10^{-1} with high likelihood. As increasing values of the internalization rate are measured in a bio-lab experiment, the highest likelihood of the α_b parameter moves toward greater values. However, in these cases, the likelihood distribution of the α_b parameter values tends to flatten out. Thus, the inference of the parameter values given the internalization becomes more uncertain.

From Fig. 6b and Fig. 6c we can infer with high likelihood the values of the parameters b_f or b_d for each given order of magnitude of the measured internalization rate. More specifically, increasing values of the internalization rate correspond to increasing values of b_f or b_d parameters.

Fig. 6d shows that the parameter b_u has a lower impact on the internalization rate, since the likelihood distribution appears to be uniform for each value of the internalization rate. Therefore, the uncertainty about the value of such parameter remains high.

Finally, Fig. 6e shows the likelihood distribution of the ratio $\mathcal{V}_0$ for each given order of magnitude of the measured internalization rate. This information is useful to infer information about the initial concentration F_0 of FPs. In fact, as mentioned in Section II-B, the initial concentration V_0 of EVs is assigned during biological experiment planning. Therefore, through (16), the most likely values of the ratio $\mathcal{V}_0$ can be easily translated in terms of the initial concentration F_0 of proteins. The results in Fig. 6e show that the measured internalization rates in the order of 10^{-1} are with high likelihood achieved for $\mathcal{V}_0$ in the order of 10, as well as internalization rates in the order of 10^3 are with high likelihood achieved for $\mathcal{V}_0$ in the order of 10^5. However, for intermediate values of the internalization rates, the inference of $\mathcal{V}_0$ values is performed with great uncertainty.

IV. CONCLUSIONS

In this paper we have considered the communication between biological cells through the exchange of EVs. More specifically, we have modeled the processes and functionalities of the cells as receiving devices, focusing on EV internalization through their fusion to the plasma membrane of the target cell as receiving mechanism. We have derived a mathematical model which describes the fusion process through a system of ordinary differential equation.

Since little information is available in literature about the values of the biological parameters regulating the fusion process, a deep investigation on the impact of the model parameters on the evolution of the process has been carried out by evaluating the numerical solution of the model for a wide range of parameters values. Further, we have provided a frame of reference for future comparisons between numerical solutions and biological experimental measures. Finally, we have used the model as a tool to infer the range of most likely values for these biological parameters, given some common bio-lab measurements, such as the EV internalization rate in the receiving cell.

As shown in the paper, a future application of the model presented in this work, is its use as a tool, for deriving the values of biological parameters, such as the rate constants summarized in Table I, that are not directly measurable in labs, from the measure of the EV concentration in different phases of the process, such as the concentration of available EVs in the extracellular medium or the ones inside the cell. Moreover, once the parameters of interested are determined, the use of the model can be extended to the design of targeted experiments. In fact, studying and analyzing the experimental scenarios to be produced beforehand, and anticipating the results to be expected, can improve the usage of experimental resources dramatically. More specifically, biological experiments testing the use of EVs for therapeutic purposes, as for other types of drug administration, require several steps of optimization, including the dose, the time and the duration of the administration, and the necessity of eventual boosts. This makes them often expensive and time consuming, and makes it difficult to perform all the preliminary studies needed to find the optimum parameters. In this context, the model allows to forecast the results of planned experiments and to design accordingly the experiments to be performed, without waste of resources and time. As an example, the model allows to calculate the concentration of EVs to be administered in order to guarantee a desired concentration of EVs in a given time interval. To find this value without the model, several experiments must be conducted for diverse concentration of the administered EVs, until the desired value is achieved. Obviously, this second case produces a waste of resources and time, that the use of the model allows to avoid.

REFERENCES

[1] I. F. Akyildiz, M. Pierobon, S. Balasubramaniam, and Y. Koucheryavy. The internet of bio-nano things. *IEEE Communications Magazine*, 53(3):32–40, 2015.

[2] B. Bjerregaard, J. Lemmen, M. Petersen, E. Østrup, L. Iversen, K. Almstrup, L.-I. Larsson, and S. Ziebe. Syncytin-1 and its receptor is present in human gametes. *Journal of assisted reproduction and genetics*, 31(5):533–539, 2014.

[3] R. Buslei, P. L. Strissel, C. Henke, R. Schey, N. Lang, M. Ruebner, C. C. Stolt, B. Fabry, M. Buchfelder, and R. Strick. Activation and regulation of endogenous retroviral genes in the human pituitary gland and related endocrine tumours. *Neuropathology and Applied Neurobiology*, 41(2):180–200, 2015.

[4] L. Cheng and A. Hill. Therapeutically harnessing extracellular vesicles. *Nature Reviews Drug Discovery*, 21:1–21, 03 2022.

[5] J. Duman, E. Lee, G. Lee, G. Singh, and J. Forte. Membrane fusion correlates with surface charge in exocytic vesicles. *Biochemistry*, 43(24):7924–7939, 2004.

[6] S. El Andaloussi, I. Mäger, X. O. Breakefield, and M. J. Wood. Extracellular vesicles: biology and emerging therapeutic opportunities. *Nature reviews Drug discovery*, 12(5):347–357, 2013.

[7] J.-M. Galan, A. Wiederkehr, J. H. Seol, R. Haguenauer-Tsapis, R. J. Deshaies, H. Riezman, and M. Peter. Skp1p and the f-box protein rcy1p form a non-scf complex involved in recycling of the snare snc1p in yeast. *Molecular and cellular biology*, 21(9):3105–3117, 2001.

[8] J. Gerst. Snares and snare regulators in membrane fusion and exocytosis. *Cellular and Molecular Life Sciences CMLS*, 55:707–734, 1999.

[9] D. Guimarães, A. Cavaco-Paulo, and E. Nogueira. Design of liposomes as drug delivery system for therapeutic applications. *International journal of pharmaceutics*, 601:120571, 2021.

[10] I. Herrmann, M. Wood, and G. Fuhrmann. Extracellular vesicles as a next-generation drug delivery platform. *Nature Nanotechnology*, 16:1–12, 07 2021.

[11] B. J. Jurgielewicz, Y. Yao, and S. L. Stice. Kinetics and specificity of hek293t extracellular vesicle uptake using imaging flow cytometry. *Nanoscale research letters*, 15:1–11, 2020.

[12] V. Knecht and S.-J. Marrink. Molecular dynamics simulations of lipid vesicle fusion in atomic detail. *Biophysical Journal*, 92(12):4254–4261, 2007.

[13] L. Leggio, F. L'Episcopo, A. Magrì, M. J. Ulloa-Navas, G. Paternò, S. Vivarelli, C. A. Bastos, C. Tirolo, N. Testa, S. Caniglia, et al. Small extracellular vesicles secreted by region-specific astrocytes ameliorate the mitochondrial function in a cellular model of parkinson's disease. *bioRxiv*, 2021.

[14] L. Leggio, G. Paternò, S. Vivarelli, F. L'Episcopo, C. Tirolo, G. Raciti, F. Pappalardo, C. Giachino, S. Caniglia, M. F. Serapide, B. Marchetti, and N. Iraci. Extracellular vesicles as nanotherapeutics for parkinson's disease. *Biomolecules*, 10(9), 2020.

[15] A. Lombardo, G. Morabito, C. Panarello, and F. Pappalardo. Modeling biological receivers: The case of extracellular vesicle fusion to the plasma membrane of the target cell. In *Proceedings of the 9th ACM International Conference on Nanoscale Computing and Communication*, NANOCOM '22, New York, NY, USA, 2022. Association for Computing Machinery.

[16] P. Maliniemi, M. Vincendeau, J. Mayer, O. Frank, S. Hahtola, L. Karenko, E. Carlsson, F. Mallet, W. Seifarth, C. Leib-Mösch, et al. Expression of human endogenous retrovirus-w including syncytin-1 in cutaneous t-cell lymphoma. *PloS one*, 8(10):e76281, 2013.

[17] K. J. McKelvey, K. L. Powell, A. W. Ashton, J. M. Morris, and S. A. McCracken. Exosomes: mechanisms of uptake. *Journal of circulating biomarkers*, 4:7, 2015.

[18] L. A. Mulcahy, R. C. Pink, and D. R. F. Carter. Routes and mechanisms of extracellular vesicle uptake. *Journal of extracellular vesicles*, 3(1):24641, 2014.

[19] B. Podbilewicz. Virus and cell fusion mechanisms. *Annual review of cell and developmental biology*, 30:111–139, 2014.

[20] A. Pötgens, S. Drewlo, M. Kokozidou, and P. Kaufmann. Syncytin: the major regulator of trophoblast fusion? recent developments and hypotheses on its action. *Human reproduction update*, 10(6):487–496, 2004.

[21] I. Prada, L. Amin, R. Furlan, G. Legname, C. Verderio, and D. Cojoc. A new approach to follow a single extracellular vesicle—cell interaction using optical tweezers. *BioTechniques*, 60(1):35, 2016. PMID: 26757810.

[22] I. Prada and J. Meldolesi. Binding and fusion of extracellular vesicles to the plasma membrane of their cell targets. *International journal of molecular sciences*, 17(8):1296, 2016.

[23] A. E. Russell, A. Sneider, K. W. Witwer, P. Bergese, S. N. Bhattacharyya, A. Cocks, E. Cocucci, U. Erdbrügger, J. M. Falcon-Perez, D. W. Freeman, et al. Biological membranes in ev biogenesis, stability, uptake, and cargo transfer: an isev position paper arising from the

isev membranes and evs workshop. *Journal of Extracellular Vesicles*, 8(1):1684862, 2019.

[24] T. Tian, Y.-L. Zhu, F.-H. Hu, Y.-Y. Wang, N.-P. Huang, and Z.-D. Xiao. Dynamics of exosome internalization and trafficking. *Journal of Cellular Physiology*, 228(7):1487–1495, 2013.

[25] J. Tolosa, J. Schjenken, V. Clifton, A. Vargas, B. Barbeau, P. Lowry, K. Maiti, and R. Smith. The endogenous retroviral envelope protein syncytin-1 inhibits lps/pha-stimulated cytokine responses in human blood and is sorted into placental exosomes. *Placenta*, 33(11):933–941, 2012.

[26] T. D. Vance and J. E. Lee. Virus and eukaryote fusogen superfamilies. *Current Biology*, 30(13):R750–R754, 2020.

[27] A. Vargas, S. Zhou, M. Éthier-Chiasson, D. Flipo, J. Lafond, C. Gilbert, and B. Barbeau. Syncytin proteins incorporated in placenta exosomes are important for cell uptake and show variation in abundance in serum exosomes from patients with preeclampsia. *The FASEB Journal*, 28(8):3703–3719, 2014.

[28] M. Veletić, M. T. Barros, I. Balasingham, and S. Balasubramaniam. A molecular communication model of exosome-mediated brain drug delivery. In *Proceedings of the Sixth Annual ACM International Conference on Nanoscale Computing and Communication*, pages 1–7, 2019.

[29] M. Veletić, M. T. Barros, H. Arjmandi, S. Balasubramaniam, and I. Balasingham. Modeling of modulated exosome release from differentiated induced neural stem cells for targeted drug delivery. *IEEE Transactions on NanoBioscience*, 19(3):357–367, 2020.

[30] H. C. Verdera, J. J. Gitz-Francois, R. M. Schiffelers, and P. Vader. Cellular uptake of extracellular vesicles is mediated by clathrin-independent endocytosis and macropinocytosis. *Journal of Controlled Release*, 266:100–108, 2017.

[31] F. Verweij, L. Balaj, C. Boulanger, D. Carter, E. Compeer, G. D'Angelo, S. Andaloussi, J. Goetz, J. Gross, V. Hyenne, E.-M. Krämer-Albers, C. Lai, X. Loyer, A. Marki, S. Momma, E. Hoen, D. Pegtel, H. Peinado, G. Raposo, and G. Niel. The power of imaging to understand extracellular vesicle biology in vivo. *Nature Methods*, 18:1–14, 08 2021.

[32] S. Vivona, D. J. Cipriano, S. O'Leary, Y. H. Li, T. D. Fenn, and A. T. Brunger. Disassembly of all snare complexes by n-ethylmaleimide-sensitive factor (nsf) is initiated by a conserved 1: 1 interaction between α-soluble nsf attachment protein (snap) and snare complex. *Journal of Biological Chemistry*, 288(34):24984–24991, 2013.

[33] J. Wattis, B. O'Malley, H. Blackburn, L. Pickersgill, J. Panovska, H. Byrne, and K. Jackson. Mathematical model for low density lipoprotein (ldl) endocytosis by hepatocytes. *Bulletin of mathematical biology*, 70(8):2303–2333, 2008.

[34] M. Zoofaghari, F. Pappalardo, M. Damrath, and I. Balasingham. Modeling extracellular vesicles-mediated interactions of cells in the tumor microenvironment. *IEEE Transactions on NanoBioscience*, pages 1–1, 2023.

Alfio Lombardo received his degree in electrical engineering from the University of Catania, Italy, in 1983. Until 1987, he acted as consultant at CREI, the center of the Politecnico di Milano for research on computer networks, where he was involved as technical leader in various European projects. In 1988 he joined the University of Catania where he is full professor of Internet (SSD.: ING-INF/03). From 1996 to the present he has been the leader of the University of Catania team in several European and/or national projects. In 2005 he founded a company as a research spin off of the Informatics and Telecommunication Department in the University of Catania; he was the scientific coordinator of both the OpenLab and Riltus laboratories. He was the Catania team leader of the CNIT (Consorzio Nazionale Interuniversitario per le Telecomunicazioni) research unit. His research interests include network modeling analysis, multimedia, green networking, microfluidic networks, intrabody communication systems. He is author of more than 170 papers on these subjects.

Giacomo Morabito received the laurea degree in Electronic Engineering and the PhD in Electrical, Computer, and Telecommunications Engineering from the Istituto di Informatica e Telecomunicazioni of the University of Catania (Italy), in 1996 and 2000, respectively. From November 1999 to April 2001, he was with the Broadband and Wireless Networking Laboratory of the Georgia Institute of Technology as a Research Engineer. Since April 2001 he is with the Dipartimento di Ingegneria Elettrica Elettronica e Informatica of the University of Catania where he is currently full professor of Telecommunications. His research interest focuses on modeling and design of communication networks and systems.

Carla Panarello Carla Panarello received the Laurea Degree in Electronics Engineering and the PhD in Computer and Telecommunication Engineering, from the University of Catania, Italy, in 2004 and 2010, respectively. From October 2005 to May 2006, she was involved in a research collaboration with CNR about congestion control and performance optimization in TCP/IP networks. From September to November 2006, she has been a visiting student at the Network Research Lab, Computer Science Department, UCLA. From 2010 to 2012, she worked as a Research Fellow with the Italian National Consortium of Telecommunications (CNIT), on green networking within the TREND (Towards Real Energy-efficient Network Design) project. Currently, she is a Post Doctoral Researcher at the University of Catania. Her research interests include design, modeling and performance analysis of communication networks, green networking, microfluidics, molecular and intercellular communications.

Fabrizio Pappalardo received the Bachelor's Degree in Biological Sciences in 2018 and the Master's Degree in Medical Biotechnology in 2020 from the University of Catania, Italy. Since 2020 he has been working in the field of molecular communication and assessment of microfluidic devices. Currently he is a PhD. student at the Department of Electrical, Electronics and Computer Engineering of the University of Catania.